

and K. H. Johnson, *J. Chem. Phys.* **61**, 3508 (1974).

¹³See for example, G. D. Watkins and R. P. Messmer, in *Computational Methods for Large Molecules and Localized States in Solids*, edited by F. Herman *et al.* (Plenum, New York, 1973), p. 133.

¹⁴A. B. Anderson and R. Hoffman, *J. Chem. Phys.* **61**, 4545 (1974); I. P. Batra and O. Robaux, *J. Vac. Sci. Technol.* **12**, 242 (1975).

¹⁵G. D. Watkins and R. P. Messmer, *Phys. Rev. Lett.* **32**, 1244 (1974).

¹⁶*Handbook of Chemistry and Physics*, edited by R. C. Weast (Chemical Rubber Company Press, Cleveland, Ohio, 1972-1973), 53rd ed., pp. F-183, F-184.

¹⁷E. O. Kane, *Phys. Rev.* **146**, 558 (1966).

¹⁸E. Tosatti and P. W. Anderson, *Jpn. J. Appl. Phys., Suppl.* **2**, 381 (1974).

Sputtering of Nb and Au by (*d, t*) Neutrons*

O. K. Harling, M. T. Thomas, R. L. Brodzinski, and L. A. Rancitelli

Pacific Northwest Laboratory of the Battelle Memorial Institute, Richland, Washington 99352

(Received 17 March 1975)

Neutron-sputtering ratios are reported for (*d, t*) neutrons incident upon Nb and Au foils. The measured ratios are lower than most previous results. For annealed Au as well as for cold-worked Nb the best values for the sputtering ratios are in the range $S_n \approx (1.2-2.5) \times 10^{-5}$. These results are in good agreement with theoretical predictions. A careful search for neutron-induced micron-sized particles yielded negative results.

Neutron-sputtering ratios have been measured by various experimenters¹⁻¹²; however, the results are in poor agreement and are generally higher than ratios predicted by theory.¹³⁻¹⁵ Exceptionally high fast-neutron yields have been observed by Kaminsky and Das^{8,9}; they report sputtering ratios as high as 0.25 ± 0.1 atoms per (*d, t*) neutron for cold-worked Nb foils. The sputtered material at these high yields was observed to be primarily in the form of micrometer-sized chunks. Guinan¹⁶ has developed a theory to explain neutron-triggered emission of chunks on the basis of stored internal energy. However, a theoretical treatment by Weertman¹⁷ questions the possibility that micron-sized chunk emission can be caused by fast neutrons at the fluence levels used in Kaminsky and Das's experiment.

In summary, the available experimental results and the theoretical predictions of neutron-sputtering ratios, cited above, range over four orders of magnitude. That is, from $S_n \approx 10^{-5}$, according to theory, to $S_n > 10^{-1}$, according to some experiments. At the present time it appears difficult to postulate theoretical mechanisms to explain the highest measured sputtering ratios and the associated micron-size particle emission.

In this paper we report some results for Au and Nb following an extensive series of (*d, t*)-neutron-sputtering experiments on various metals and nonmetals. Figure 1 shows the general arrangement of our sputtering targets, collectors,

and the (*d, t*)-neutron source. All measurements reported here were made at the Lawrence Livermore Laboratory using their rotating target neutron source (RTNS). The neutrons were produced in a thin tritiated Ti target which was bombarded with 400-keV D^+ ions. A source strength of $(3-5) \times 10^{12}$ neutrons/sec was attained in a source spot of $\sim 1 \text{ cm}^2$.

Targets were prepared from high-purity commercially available materials such as Materials Research Corporation, Marz-grade Nb. Most collectors or catchers for sputtered material

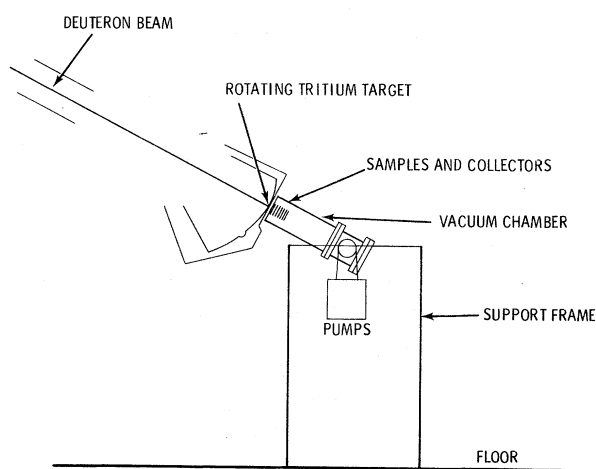


FIG. 1. Experimental arrangement at the (*d, t*)-neutron source.

were made from nominal 99.999 999 9+%-purity silicon single crystal or polycrystal material which was cut into the form of thin wafers 2.54 cm in diameter and about 0.075 cm thick and was then optically polished. Neutron-sputtering targets were prepared with various treatments: some were highly cold worked (CW), some were vacuum annealed, some were mechanically polished and electropolished, and some were chemically etched. In this Letter data for cold-worked niobium and annealed gold will be presented.

Acid etching and ultrasonic cleaning in baths of solvent and deionized, doubly distilled water were generally used for cleaning of targets and collectors as well as mounts. All final cleaning and assembly operations were carried out in clean-air hoods and with clean-room techniques to minimize environmental contamination. Every target or collector was independently mounted in a high-purity aluminum ring. Some catchers were split vertically to provide separate samples for neutron-activation analysis (NAA) and for scanning-electron-microscope (SEM) analysis. The sample-collector stack was held in a stainless-steel tube which was inserted into an all-metal vacuum system and given a mild bake at $\approx 150^\circ\text{C}$. After cooling the stack was transferred, under dry argon or nitrogen, to a stainless-steel transfer chamber for shipment to the (d, t) -neutron source. All transfers were done in filtered-gas environments.

At the RTNS the sample is transferred to the vacuum irradiation apparatus, and the irradiation carried out as shown schematically in Fig. 1. Irradiations with RTNS neutrons are made with (d, t) neutrons emitted from the target in the forward direction. The mean energy¹⁸ of the neutrons striking the sputtering sample is ≈ 14.8 MeV. Temperature during irradiation is believed to be near room temperature. The pressure in the irradiation chamber is in the range 10^{-6} – 10^{-8} Torr for these experiments. Irradiations were made for beam-on-time periods of 16–45 h. This irradiation time provided fluences in the range 5×10^{14} to 2.6×10^{16} (d, t) neutrons/cm².

Following RTNS irradiation the sample stack is transferred from the irradiation apparatus under clean conditions, and shipped under a clean N₂ or Ar environment in a stainless-steel container. After arrival at our laboratory, the sample stack is unloaded and disassembled in a laminar flow of absolute filtered air. Following stack disassembly, several types of analyses are car-

ried out. Nuclear counting on dosimetry foils of Nb, Ni, V, and Al establishes the (d, t) -neutron dose for each target. Collectors which are to be assayed for total yields of nonradioactive sputtered target material are activated in a reactor and then counted for induced activity. In the case of Nb we count the ^{94m}Nb by x-ray counting of the 6.29-min activity following a rapid chemical separation¹⁹ of the Nb which removes it from the collector surface and decreases contamination from other elements. A number of internal cross checks and calibrations are used to determine the chemical yields, which average $\sim 87\%$, and to establish the absolute detection sensitivity for the NAA for each sample. Measurement of the gold yields is done by singles counting of the 411-keV γ ray of ^{198}Au , following reactor activation in a thermal-neutron flux. Corrections are made for losses due to the target-collector geometry. Because of the small spacing, typically 1–2 mm, these losses are a small 5–20%. It should be emphasized that the assay by NAA is an integral and absolute measure of all the material of one element which is collected on the catchers. Sputtered metal, whether in the form of atomic deposits or micron-sized chunks, can be accurately assayed by this technique.

Scanning-electron-microscope analysis was carried out for several collectors which faced Nb targets during the (d, t) irradiation. During SEM analysis a systematic survey was made of the surface of the polished single-crystal Si wafers used as sputtering collectors. Scanning is done at 300 \times and 1000 \times in the secondary-electron-detection mode. Whenever any indication of a particle is found, the electron beam is focused on the particle with high magnification, and x-ray analysis using an energy-dispersive crystal detector is carried out. SEM analysis has emphasized coverage of the lower part of our collectors since Kaminsky and Das^{8,9} have reported a higher probability of micron-sized chunks on the lower parts of their collectors. The manner in which we have carried out the SEM analysis of our samples makes it unlikely that we would fail to observe more than one or two particles greater than ~ 0.5 μm in the areas which are analyzed. A total area of 1 cm² was scanned at 300 \times on silicon collectors which faced two separate CW Nb targets exposed to fluences of $3.6 \times 10^{15}/\text{cm}^2$ and $1.1 \times 10^{16}/\text{cm}^2$. In addition, 1.2 cm² of the forward collector of a CW Nb target provided by M. Kaminsky was scanned at 1000 \times after irradiation.

TABLE I. (d, t) neutron sputtering yields by NAA.

Target material	Range of S_n values	
	Forward sputtering	Backward sputtering
Gold ^a	2.5×10^{-5} to 4.5×10^{-4}	1.2×10^{-5} to 2.0×10^{-4}
Nb I ^{b, c}	1.1×10^{-5} to 5.9×10^{-4}	1.5×10^{-5} to 1.3×10^{-3}
Nb II ^{b, d}	6.4×10^{-5} to $< 2.3 \times 10^{-4}$	$< 4.4 \times 10^{-5}$ ^g to $< 1.0 \times 10^{-3g}$
Nb III ^{b, e}	$< 3.6 \times 10^{-5g}$	8.5×10^{-4}
Nb IV ^{b, f}	SEM only	$< 6 \times 10^{-5}$

^aMarz-grade material, vacuum annealed at 375°C for 1 h, etched 5 min in aqua regia; 2.54 cm diam by 0.0127 cm thick; seven separate target irradiations.

^bMarz-grade CW material, 2.54 cm diam by 0.0127 cm thick.

^cMechanically polished and electropolished (Ref. 20), surface roughness 1–5 μm ; three separate targets and one irradiation.

^dAcid etched $\sim 10 \mu\text{m}$ per surface, roughness 1–4 μm ; two separate targets, three separate irradiations.

^eFast (1 sec) acid etch, mechanically polished, 600-grit paper and 0.3- μm Al_2O_3 , roughness 1–4 μm ; one target, one irradiation.

^fFast (1 sec) etch, in equal parts of HF, HNO_3 , and H_2O after optical grinding to a finish of approximately 5 μm . Sample from and preparation by M. Kaminsky.

^gThe $<$ sign implies an upper limit for S_n , i.e., no yield was measured within the sensitivity of the NAA measurement. The variation in the value of S_n following the $<$ sign reflects variations in (d, t) -neutron fluence as well as variations in the thermal-neutron flux used for the NAA.

tion to a (d, t) -neutron fluence of 5.5×10^{15} neutrons/cm². This target is representative of the targets which give high sputtering yields and chunks in the experiments of Kaminsky and Das. No niobium particles were found on any of the collectors scanned.

Neutron-sputtering ratios for annealed-gold targets and CW Nb targets with several surface preparations are presented in Table I. The range of S_n values is given where more than one measurement was made. Individual S_n values for the seven measurements on gold range from 4.5×10^{-4} to 1.2×10^{-5} . The lowest values are believed to be the most likely since gold contamination on the collectors has been found during all blank experiments.

A firm value for the neutron-sputtering ratio can be found under conditions of variable collector contamination only if sufficient measurements have been made so that S_n , the yield divided by the neutron fluence, is tending toward a constant value independent of fluence as the fluence is increased. For forward sputtering of gold we have four values of S_n in the range $(2.5-5) \times 10^{-5}$ and over a fluence range of more than a factor of 10. We therefore feel that $\approx 2.5 \times 10^{-5}$ is the most likely value for the Au forward-sputtering ratio. Similarly the lowest sputtering ratios for back-

ward Au sputtering range from $(1.2-2.5) \times 10^{-5}$ with an order of magnitude variation in fluence. We therefore feel that $\approx 1.2 \times 10^{-5}$ is the most likely value for Au backward sputtering. Similar examination of the Nb-sputtering results suggest the conclusion that the lowest measured values of S_n are the most likely. The relatively few measurements for each type of CW Nb sample, however, do not allow an extrapolation to the most likely value of S_n with the same certainty as for Au where there are seven separate experiments on the same type target. However, examination of all the Nb data taken together indicates that the most likely values for S_n are $\approx 1.5 \times 10^{-5}$ for forward and backward sputtering. The \approx in our best values for S_n reflect the uncertainty that some of the measured yield may still be due to collector contamination.

*Research performed under U. S. Atomic Energy Commission (now Energy Research and Development Administration) Contract No. AT(45-1)-1830.

¹D. W. Norcross, B. P. Fairand, and J. N. Anno, J. Appl. Phys. **37**, 621 (1966).

²K. Keller and R. V. Lee, Jr., J. Appl. Phys. **37**, 1890 (1966).

³K. Keller, Plasma Phys. **10**, 195 (1968).

⁴R. J. Garber, G. P. Dolya, V. M. Kolyada, A. A. Molden, and A. I. Federenko, *Pis'ma Zh. Eksp. Teor. Fiz.* **7**, 375 (1968) [*JETP Lett.* **7**, 296 (1968)].

⁵K. Verghese, *Trans. Amer. Nucl. Soc.* **12**, 544 (1969).

⁶R. F. Garber, V. S. Karasov, V. M. Kolyada, and A. I. Federenko, *At. Energ.* **28**, 400 (1970) [*Sov. At. Energy* **28**, 510 (1970)].

⁷T. S. Baer and J. N. Anno, *J. Appl. Phys.* **43**, 2453 (1972).

⁸M. Kaminsky, J. H. Peavey, and S. K. Das, *Phys. Rev. Lett.* **32**, 599 (1974).

⁹M. Kaminsky and S. K. Das, *J. Nucl. Mater.* **53**, 162 (1974).

¹⁰R. Behrisch, *Nucl. Fusion* **12**, 695 (1972).

¹¹M. A. Kirk, T. H. Blewitt, A. C. Klank, and T. L. Scott, *J. Nucl. Mater.* **53**, 179 (1974).

¹²R. Behrisch, R. Bahler, and J. Kalus, *J. Nucl. Mater.* **53**, 183 (1974).

¹³S. J. Taimuty, *Nucl. Sci. Eng.* **10**, 403 (1961).

¹⁴P. Sigmund, *Phys. Rev.* **184**, 383 (1969).

¹⁵M. T. Robinson, *J. Nucl. Mater.* **53**, 201 (1974).

¹⁶M. Guinan, *J. Nucl. Mater.* **53**, 171 (1974).

¹⁷J. Weertman, to be published.

¹⁸J. D. Seagrave, "D(*d,n*)He³ and T(*d,n*)He⁴ Neutron Source Handbook," LASL Report No. LAMS-2162, 1958 (unpublished).

¹⁹R. L. Brodzinski *et al.*, to be published.

²⁰M. Kaminsky and S. Das, *J. Appl. Phys.* **44**, 25 (1973).

Electronic Band Structure, Bonding, and Ionicities of Polymorphous Thallous Halides

J. Treusch

Institut für Physik der Universität Dortmund, 46 Dortmund, Germany

(Received 20 January 1975)

An empirical linear-combination-of-atomic-orbitals energy-band model is described for simple-cubic and fcc TlCl, TlBr, and TlI which explains optical data and reproduces existent *a priori* band structures. This band model is used to discuss the type of bonding in the polymorphs, and to check the applicability for ten-electron systems of the Phillips-van Vechten dielectric theory of bonding.

The Phillips-van Vechten dielectric theory (PV theory) of bonding and ionicity¹ has undoubtedly been extremely successful in the field of eight-electron systems, ranging from tetrahedrally coordinated semiconductors, for which it had been primarily intended, to crystals as ionic as the alkali halides. This success initiated several attempts to extend this theory to more complicated compounds,² including those where *d* electrons play an important role, and even to ten-electron systems like the lead chalcogenides and thallous halides.³

Recent optical measurements and band-structure calculations on the polytypes of TlCl, TlBr, and TlI,⁴ which can be grown in NaCl structure (fcc) as well as in their normal CsCl structure [simple cubic (sc)], yield an almost ideal opportunity to check whether these ten-electron compounds fit into the pattern of the PV theory. Moreover, a treatment of these rather simple systems may also help for a better understanding of other more complicated systems with a cationic *s* shell exceeding the rare-gas configuration.

The basic difference between the thallous halides and the alkali halides from our point of view is the fact that the anion *s*-type conduction band

and the cation *p*-type valence band, which in the latter case form the average gap entering the PV theory, are both occupied in thallous halides. So, what can be used as an average gap of the thallous halides is actually the distance between the mixed *s-p* valence band and the *p*-type cationic conduction band. It is not at all clear from the outset whether this "cationic" gap reproduces chemical trends in the same sense as the "charge-transfer" gap of eight-electron systems normally does. Moreover, the *s* shell of the cation is very easily deformable, leading to anomalously high values of the static dielectric constant, ϵ_0 , in all ten-electron compounds. This in addition may hinder a description in terms of the electronic dielectric constant, ϵ_∞ , alone.⁵

To make possible a description of the thallous halides, which is unambiguous, simple, and shows the essentials of why the electronic structure is as it is, an empirical linear-combination-of-atomic-orbitals (LCAO) scheme has been developed.⁶ This scheme reestablishes the band structures that have been calculated with the Korringa-Kohn-Rostoker (KKR) method for all six polymorphs and which are taken for granted since they explain optical data very satisfactorily.